REPORT NO. SR64-1006

FINAL REPORT

CONTRACT NO. NAS 2-1097

DEVELOPMENT OF AN IMPEDANCE PNEUMOGRAPH

PREPARED FOR:

NATIONAL AERONAUTICS &
SPACE ADMINISTRATION
AMES RESEARCH CENTER
MOFFETT FIELD, CALIFORNIA

PREPARED BY:

SPACELABS, INC.
15521 LANARK STREET
VAN NUYS, CALIFORNIA

MAY 28, 1964
JOB NO. 7170

SOME PRINCIPLES OF CORRECTION TABLES TO BE USED FOR EVALUATION OF THE RATE OF INFORMATION PROCESSING

[Following is the translation of an article by A. A. Genkin, V. I. Medvedev, and M. P. Shek, Military Medical Order of Lenin Academy imeni S. M. Kirov, Leningrad, in the Russian-language periodical Voprosy psikhologii (Problems in Psychology), No 1, Jan/Feb 1963, Moscow, pages 104-109.]

Among the methods elaborated in experimental physiology and psychology for the quantitative examination of attention, discrimination, perception and the like, wide use is made of various sorts of correction tables which are used in an attempt to obtain data on the state of such neural processes as excitation, internal and external inhibition, etc. The seductive aspects of these methods are their simplicity, the ease with which the data obtained can be processed and their applicability in any conditions, even those of the most complex experiment.

In ito Transl. from Vopr. Psikhologii [Moscow] No. 1, 1963 10 Jun. 1963
81-16 nfa (See N64-12504 04-16) OTS: $0.75 AS]

TABLE OF CONTENTS

		Page
1.	INTRODUCTION	1
2.	EXPERIMENTAL INVESTIGATION OF IMPEDANCE PNEUMOGRAPH MEASUREMENT	2
2.1	Rationale and Objectives	2
2.2	Apparatus	3
2.3	Electrode Placement	4
2.4	Electrode Design	6
2.5	Impedance Components	7
2.6	Long Term Monitoring	7
2.7	Conclusions	7
3.	DESIGN OF IMPROVED IMPEDANCE PNEUMOGRAPH SIGNAL CONDITIONER	8
3.1	Introduction	8
3.2	Performance Specification	9
3.3	Design	12
4.	SUMMARY	16

APPENDIX A: Circuit Diagram of Impedance Component Separation Apparatus

APPENDIX B: Circuit Diagram of Impedance Pneumograph, Dwg. 102213

APPENDIX C: Bibliography

1. INTRODUCTION

Variations in patient temperature, pulse, respiration, and blood pressure have customarily been used as clinical indicators of physiological change. It was natural that these same variables would be applied to the assessment of an astronaut's condition during hypersonic flight. But the restrictions on instrument size, weight, and encumberance imposed by the aerospace situation have greatly complicated the measurement of these old variables in their new environment. Since physiological monitoring has been important to initial space exploration, and since the physiological information imparted increases with the accuracy of the measurement used, much effort has been directed toward the development of bioinstrumentation for flight applications. Technological advance in medical electronics has produced systems that permit continuous and simultaneous measurement of many biological signals in the aerospace situation. For example, miniature temperature transducers are available which permit convenient recordings of that variable. However, it has generally been difficult, and sometimes even impossible, to obtain respiration data, particularly respiratory volume, on individuals engaged in flight operations. Many devices have been developed to facilitate this measurement and all have had some disadvantages. Chest straps which measure strain bind the wearer sufficiently to promote vertical displacement of the lungs, and hence interfere with data accuracy. In addition, they are uncomfortable. Thermistors in the nasal passages have been used, but are generally inaccurate, especially if oral breathing occurs. If the subject wears a tight fitting mask it is possible to obtain quantitative volumetric and rate data. However, the mask is precluded as a practical solution if long duration monitoring is desired. The development of a device capable of accurately measuring respiratory variables in a quantitative, convenient, and non-encumbering manner during flight would, therefore, be a valuable contribution to the progress of bioastronautics.

For a number of years it has been known that a detectable impedance change occurs across the chest during the respiratory cycle. The impedance change between two applied electrodes can be measured with an alternating current impedance bridge. The total change observed is composed of a resistive component, and a reactive component contributed by the effective capacitance of the body volume. Impedance measurement is affected by electrode size and placement, frequency of the applied signal, and the build of the test subject, among other factors. Recently, interest has been aroused in the impedance measurement as a source of respiratory information. Several research groups have published on the subject during the past few years (See Appendix C, Bibliography).

In 1961, Spacelabs instituted an independent research and development program directed toward the design and fabrication of an impedance pneumograph suitable for in-flight applications. Two different designs were evolved. They were evaluated in a series of tests. The conclusion reached was that the impedance pneumograph technique was promising but that certain limitations had yet to be overcome. The observed shortcomings related to the ability of the technique

to provide true volumetric data. Measurement errors emanated from the following sources:

(1) Changes in electrode resistance, which caused baseline shifts.

(2) Physical activity (such as raising the arms over the head) which produced movement artifacts.

(3) Individual variability between test subjects, which made calibration difficult.

Further work appeared necessary before the variables of impedance pneumograph measurement were understood well enough to permit the specification of an optimum measuring device and technique.

The present development program was undertaken to provide the necessary information, and to apply it to an improved impedance pneumograph. The program consisted of a study phase and a design phase, and culminated in a set of recommendations for optimum electrode positioning and electrode construction, and in the production of two flight-packaged pneumograph units. Both the study and design phases are described in the following report.

2. EXPERIMENTAL INVESTIGATION OF IMPEDANCE PNEUMOGRAPH MEASUREMENT

2.1 Rationale and Objectives

The trans-thoracic impedance change, ΔZ, is a complex variable dependent on frequency, current, electrode configuration and contact, and in addition on the fundamental biophysical properties of the body. Accordingly, the exact nature of the change has been difficult to define. The present study program was designed, in cognizance of investigations in progress at other research centers, as a means of contributing to the theoretical understanding of the impedance phenomenon.

The impedance change across the chest can be described mathematically as:

$$\Delta Z = \Delta R + \Delta X_c$$

where

$$X_c = \frac{1}{2\pi(freq)C}$$

i.e., the impedance change ΔZ has a resistive component, ΔR, and a reactive component, ΔX_c, caused by the body capacitance. It has been suggested that these components react differently to respiratory actions and to artifact-producing body movements. A basic objective of the

investigation was, therefore, to separate those components for individual examination. In addition, we were interested in determining:

(1) The anatomical source of the impedance change.

(2) The optimum electrode location for quantitative measurements.

(3) The best size and shape of electrodes to use.

(4) Which impedance component follows respiration more accurately.

(5) Methods for eliminating motion artifact.

(6) The volumetric correlation between measurements taken with the pneumograph and a servo spirometer.

(7) Signal changes resulting from long duration measurements.

(8) What other bioelectric variables may be simultaneously obtained using the same set of electrodes.

The direct application of the information gained was the design of an improved impedance pneumograph, and the specifications of an optimum measurement technique.

2.2 Apparatus

A specialized test instrumentation system was designed and constructed to permit the continuous recording of each of the three impedance variables: ΔZ, ΔX_c, and ΔR. This system is shown schematically in Figure 1.

The signal from a 50 kc oscillator was arranged to drive a circuit which provided a constant current to the electrode impedance. The voltage change across the electrodes was amplified, and fed to either a full-wave rectifier or a specially designed phase detector unit. The voltage output from the rectifier circuit was proportional to ΔZ, that leaving the phase detector was proportional to either ΔR or ΔX_c. Selection of a particular component was accomplished by using the original oscillator signal, either in-phase or shifted 90° as a reference signal to the phase detector. If an in-phase reference was used, the detector yielded the in-phase component of the impedance change; that is, ΔR. If a shifted reference was used, the detector yielded the imaginary component; that is, ΔX_c. Use of a constant current supply to the impedance electrodes eliminated the

need for balance adjustments, and ensured that a change in body reactance would not appreciably affect the phase of the oscillator voltage. The system was designed to provide only one voltage output; so that sequential recordings of the three variables could be made. Tests showed that the equipment provided a good separation between resistive and reactive changes of impedance. (The complete circuit diagram of this system is found in Appendix A.)

A servo spirometer manufactured by Med-Science Electronics, Inc. (Model 250) was the other major piece of test equipment. It provided a comparison standard for the impedance pneumograph measurements. A conventional complement of oscilloscopes, recorders, etc., constituted the supplementary test equipment. In addition, a standard tilt-table was used to produce variations in subject orientation for some of the tests.

2.3 Electrode Placement

The body was mapped to determine the optimum electrode sites for impedance pneumograph measurement. Figure 2 illustrates the site locations examined; the sites shown shaded represent impedance measurements taken through the chest (that is, from front to back). Prior to measurement, commercial electrode paste was rubbed on the skin, and 5/8" diameter gold-plated disc electrodes were taped into place. Electrode impedance was found to range between 250 and 380 ohms at 50 kc. Recordings were made showing changes in total impedance, and in the resistive and capacitive components. For comparative purposes the respiratory wave form was recorded with a servo spirometer.

Initially, complete tests were conducted on two subjects in order to compare the amplitude of artifacts generated by extraneous movement to the amplitude of the normal respiratory curve. Artifact deflections were recorded during the following activities:

(1) Raising arms over head at the side.

(2) Raising arms over head in front.

(3) Walking up two steps.

(4) Push-ups.

(5) Rotation on tilt-table through a 180° arc starting in the vertical position.

Figure 3 presents typical records obtained on one subject during normal respiration, and while he was sustaining an inhalation and raising his arms over his head in front of his body. Three arm movements are shown on

each record. However, as previously explained, the recordings were not taken simultaneously and thus represent successive runs.

After the initial tests, five different subjects were instrumented at those sites which provided the strongest signal output. From these additional runs, it was found that:

(1) Location of the electrodes on the extremities proved unsatisfactory for measuring respiration.

(2) Sensitivity was greater at locations 1 and 5 than at 4, 6, 7, 10, and 12.

(3) No respiratory signal was detected at position 7.

(4) Positions 2, 3, 8, and 9 provided good respiration signals although the sensitivity was less than at 1 or 5.

It was observed that with some subjects the impedance changes measured at locations 1, 5, 11, or 13 did not maintain a consistent relation to the respiratory events. This phenomenon is illustrated in Figure 4. As seen the ΔZ trace moves upward as the spirometer trace moves upward and falls as the spirometer trace falls. But as the spirometer trace reaches its minimum position, ΔZ reverses, and briefly moves upward again. Figure 5 shows how this change in direction corrected itself as the subject was moved to a horizontal position on the tilt-table. With the tilt-table at 45°, the reversal phenomenon is still present; at 90°, it has disappeared.

These observations seemed to indicate that the impedance measurement was materially affected by the changing position of the viscera during respiration.

In view of the electrode sites involved, it appeared that the liver was a major contribution. To test this hypothesis, electrodes were placed at the ninth rib on the right side, and at the sixth rib on the right side, and at the sixth rib on the left side, so as to include the top of the liver in the line between them. The liver is a high-density mass, and accordingly should present a low impedance pathway. It was reasoned that if a subject held his breath and raised his arms, the resulting upward movement of the liver should lower the measured impedance between the selected electrode sites.

Figure 6 reproduces a record bearing out this supposition. The second arm raising episode, with the arms raised in front of the body, gives a clearer indication of the results. As the arms are raised three times, three definite drops in impedance occur. The same data was obtained for all five subjects, but the electrode placement was different for each, indicating that liver position differs somewhat among individuals.

It was concluded from these tests that movement artifact could be reduced if the impedance electrodes included a substantial chest volume, but were across the top of the liver. Several such electrode positions were examined. The location which produced the most stable and repeatable signals utilized one electrode in the middle of the back at the second lumbar vertebrae and the other on the right side at the mid-auxillary line between the seventh and eighth ribs. The exact position of the latter electrode had to be varied with the individual and the relative position of the liver. Figure 7 shows a typical recording using this electrode placement. As seen, the respiratory movements are clearly defined, but the deflections due to arm movement are quite small. Thus, it appeared that electrode placement across the top of the liver offered a better measurement approach than placing the electrodes directly opposite each other on the chest.

2.4 Electrode Design

The following types of electrodes were procured or fabricated, and were tested to determine the one most suitable for long-duration impedance monitoring:

(1) Gold-plated disc - 5/8' diameter.

(2) Stainless steel screen - 5/8" diameter.

(3) Silver-silver chloride - 5/8" diameter.

(4) Silver-silver chloride - 3/8" diameter.

(5) Silver - 5/8" diameter.

(6) Silver with sponge insert - 5/8" diameter.

The silver electrode with a sponge insert produced the best results. Figure 8 illustrates the construction of this electrode.

The electrode shell was prepared from silastic rubber; the attached Stomaseal ring provided adhesion to the skin. An open-cell plastic sponge with a center hole was cut to fit the well in the electrode shell. The sponge was moistened in water, squeezed out, and then placed moist into a container of Burdick Electrode Paste. It absorbed sufficient paste to ensure good conduction. When the electrode was applied to the skin, the hole in the sponge prevented excess paste from being squeezed out under the lip of the electrode shell. Test results indicated that a silver-silver chloride base offered no advantage over pure silver in this configuration. Similarly, changes in electrode size had a negligible effect aside from influencing the convenience of application.

2.5 Impedance Components

Further investigations of the impedance components during respiration and body movements were undertaken on five subjects, using the preferred electrodes and electrode position. Figure 9 presents records obtained while the subject raised his arms over his head. It may be observed that ΔR increases as the arms are raised, while ΔX_c decreases. The effect on ΔZ is indeterminant here. Much the same result is also seen in the records of Figure 10. Figure 10 shows that the typically larger magnitude of the ΔR trace is clear. The ΔZ trace is clear. The ΔZ trace responds much less to the artifact-producing motion, particularly during the sustained inhalation.

It was concluded from the tests conducted that the impedance changes observed were a combination of two components. While ΔZ was generally somewhat smaller in amplitude than the resistive component, it appeared to be less subject to movement artifact. It was, therefore, decided that ΔZ should be used as an indicator of respiration. Figure 11 illustrates the good correlation between respiration recorded with the impedance pneumograph and respiration simultaneously recorded with the servo spirometer. It is interesting to note that the impedance measurement has a significantly shorter response time.

2.6 Long Duration Monitoring

The sponge electrodes were worn for 24 hours by a test subject. Electrode impedance at the start of the test was 320 $\angle -36°$ ohms. At the end of the test, it had changed to 350 $\angle -31°$ ohms. The impedance pneumograph record obtained after 24 hours appeared quite normal.

2.7 Conclusions

The conclusions derived from the experimental study are summarized below.

(1) The impedance change associated with the respiratory cycle is caused mainly by the shifting of the viscera. Since the liver is the largest and densest homogeneous body subject to these movements, it is responsible for the major portion of the impedance change.

(2) Artifact due to movement of the subject can be minimized by careful placement of the electrodes with respect to the liver.

(3) The sponge insert silver disc electrodes offer some definite advantages for impedance measurement. They produce minimal movement artifact, and exhibit excellent stability over periods up to 24 hours.

(4) Impedance (ΔZ) is less susceptable to motion artifact than either ΔR or ΔX_c and is, therefore, most easily calibrated for volumetric determinations.

(5) Because the best electrode position for impedance measurement is across the liver, it is not practical to take ECG with the same set of electrodes. However, if respiration rate only is desired, it would be possible to place the electrodes across the chest to obtain the ECG with the same set of electrodes.

(6) Although reasonable volumetric correlations between the impedance measurement and the servo spirometer could be obtained under good recording conditions, at the present time it appears that for long term monitoring of active subjects, the impedance pneumograph is limited to providing respiratory rate information and a fairly stable waveform representative of the respiratory profile.

3. DESIGN OF IMPROVED IMPEDANCE PNEUMOGRAPH SIGNAL CONDITIONER

3.1 Introduction

The results of the study program formed the basis for the design of an improved impedance pneumograph. Factors which influenced the design, but were not part of the study program, were parameters such as supply voltages, method used to couple the respiration system to the recorder (a.c. coupled or d.c. coupled) and various other detailed requirements which are covered in Section 3.2 of the Performance Specification. Much additional information relative to optimum operating frequency, etc., can be obtained in the published articles of other experimentors (reference Appendix C, Bibliography).

Earlier sections of this report pointed out that movement of the viscera was one of the primary causes of the impedance change which occurs during respiration. It has been observed that the movement of the viscera appears to have hysteresis; i.e., the viscera does not always return to the same position after body movement as it had before the movement started. This hysteresis results in a finite change in the basic impedance. Other factors which cause changes in the basic impedance are electrode movement with respect to the skin, the length of time the electrodes have been applied, the environmental temperature surrounding the test subject, and posture. It is easy to demonstrate that gross changes in baseline impedance result from changes in posture of the test subject. This change of impedance can be related directly to changes in the position of the viscera. As an illustration, if the test subject's basic impedance is measured while sitting in a chair with back straight and hands folded in lap it might typically be approximately 350 ohms at an angle of -30°. The ΔZ corresponding to shallow breathing could easily range from 0.1 to 1 ohm and the ΔZ resulting from maximum air exchange could vary between 1 and 15 ohms depending upon the physical size of the test subject. However,

in a slouched position the basic impedance could easily change from 350 ohms while sitting upright to approximately 300 ohms in the slouched position with the ΔZ reduced correspondingly as a result of change in posture. Similar results can be obtained with the test subject strapped to a tilt-table where the force of gravity acts upon the mass of the viscera. However, under space environment, the posture of the astronaut would be one of the primary factors contributing to basic impedance changes since in the "zero g" environment there would be no relative change in the position of the viscera other than that caused by muscular contraction.

The ability to obtain good respiration data using the impedance pneumograph technique is dependent upon many factors, of which the greater share cannot be improved by electronic design. A few examples are the selection of electrodes, adequate skin preparation prior to electrode application, the choice of electrode position, and assurance that a tight bond is obtained between the electrode holder and the body and evaporation or absorption of the electrolyte.

It has been observed that if the electrode diameter is in excess of 3/8 of an inch, the basic impedance does not vary appreciably between different types of electrodes. Basic impedance has been found to be related to the physical build of the subject. This impedance changes as a function of respiration and is directly related to the volume of the thoracic cavity. Stocky subjects tend to have relatively smaller changes in ΔZ for equivalent respiration than slender subjects. Tests clearly indicate that the basic impedance increases as the area of the electrode is reduced. This increase in basic impedance is accompanied by a reduction in the magnitude of the impedance change for a given volume of air exchanged.

Due to the nature of the measurement, the design of an improved impedance pneumograph signal conditioner must be based upon a compromise of conflicting requirements and should be capable of reasonable performance regardless whether the design parameter is physical, anatomical, or electronic in nature. The two pneumograph signal conditioners delivered should prove to be very useful in obtaining respiratory data under many conditions of non-optimum environment. The basis for the design of these units was established by the requirements of a performance specification.

3.2 Performance Specification

Following the conclusion of the test program, a preliminary specification for the pneumograph signal conditioner was prepared and reviewed with NASA's technical personnel. As a result of these discussions, the following specification was adopted.

3.2.1 Scope

This specification defines the requirements for a signal conditioner amplifier to operate in conjunction with suitably placed electrodes as an impedance pneumograph.

3.2.2 Requirements

3.2.2.1 Input Impedance: 10 k ohms min. at 50 kc
1 M ohm min. at 0-100 cps

3.2.2.2 Electrode Excitation: 50 kc ± 5 kc (nominal
35 mv across 286 -j 110 ohms)

3.2.2.3 Output Impedance: 1000 ohms maximum

3.2.2.4 Transfer Characteristics:

A mode switch and gain adjustment shall provide the following:

a) Direct coupled mode:

$$\frac{Eo}{\Delta Z} : \frac{1}{9} \text{ volt/ohm min.}$$

$$\frac{1}{3} \text{ volt/ohm max.}$$

where $0 \leq Eo \leq 5$ VDC

b) A.C. coupled mode:

Zero signal output voltage: +2.5 VDC ±5%

$$\frac{\Delta Eo}{\Delta Z} : \frac{1}{9} \text{ volt/ohm min.}$$

$$\frac{1}{3} \text{ volt/ohm max.}$$

for $Eo = 2.5 \pm 2.5$v

$\Delta Z = \pm 15$ ohms max.

3.2.2.5 Frequency Response

a) Direct coupled mode:

d.c. to 10 cps (-3 db at 10 cps)

b) A.C. coupled mode:

0.032 cps to 10 cps (-3 db at 0.032 cps and 10 cps)

3.2.2.6 Linearity

± 5% of maximum output

3.2.2.7 Zero set adjustment (direct coupled mode):

2.5 VDC for electrode impedances of 280 to 320 ohms.

3.2.2.8 Temperature Range (operating):

D.C. Mode: 50°F to 100°F
A.C. Mode: 32°F to 130°F

3.2.2.9 Drift (operating temperature range):

D.C. Mode: + 0.6 v maximum
A.C. Mode: ∓ 0.1 v maximum

3.2.2.10 Gain Stability (A.C. or D.C. Mode):

60°F to 100°F: + 5%
32°F to 130°F: ∓ 10%

3.2.2.11 Power

+28 ± 2.8 VDC @ 50 ma maximum

3.2.2.12 Size

4.5 cubic inches
9/16 x 2-1/8 x 3-3/4 inches

3.2.2.13 Connector

Cannon MD-1-9SL2 (Mating Connector: Cannon MD-1-9PL2)

3.3 Design

The performance specification of Section 3.2 provides a basis for the design of an impedance pneumograph signal conditioner. A requirement of the performance specification which was very difficult to provide was the capability of either a.c. or d.c. mode of operation. A.C. operation is obtained by capacitive coupling the detected carrier signal to the input of a d.c. amplifier which is the last stage in the unit. This mode of operation is conventional and does not present any difficulty. The d.c. mode, however, is not as easily obtainable in a unit which has the same order of output stability as that produced in the a.c. mode. The design problems associated with d.c. mode of operation is discussed below.

An impedance pneumograph is a device which measures the change in thoracic impedance (ΔZ) during respiration and produces an electrical output signal which is proportional to this change. The conventional method of producing an output signal proportional to the change in thoracic impedance is by exciting the pneumograph electrodes with a fairly high frequency (50 kc) constant current generator and detecting the resulting modulated carrier signal generated by the change in impedance across the electrodes. (Care must be taken to ensure that the voltage applied across the thoracic cavity does not exceed a safe maximum (0.5 volt peak-to-peak) to preclude the causing of cardiac fibrillation. An established safe operating voltage is approximately 100 mv peak-to-peak across 350 ohms resistance. At this excitation level, as the electrode impedance rises toward the design limit of 600 ohms, the electrode voltage remains at a safe level.) The electrode voltage is then amplified and peak-detected where the modulation component is separated from the carrier signal. If the electrode signal is assumed to be 100 mv peak-to-peak across 350 ohms in the absence of respiration, the electrode current is:

$$i_e = \frac{100 \times 10^{-3}}{350} = 0.286 \text{ ma peak-to-peak}$$

The required amplifier gain can be calculated for the largest electrode impedance change which corresponds to the maximum output signal.

$$A = \frac{(k_1)(k_2)\, e_o}{i_e\, (\Delta Z)}; \quad \begin{array}{l} \Delta Z \text{ max} = 15 \text{ ohm} \\ e_o \text{ max} = 5 \text{ v p-p} \end{array}$$

k_1 = 2 (conversion from peak-to-peak-to-peak)

k_2 = 2 (design factor for summing network)

Therefore,

$$A_T = \frac{20}{15(0.286 \times 10^{-3})} = 4.66 \times 10^3$$

A_T = total pneumograph gain

This carrier amplifier gain (A^1) can be determined if the d.c. gain is established ($A_{dc} \approx 40$).

$$A^1 = \frac{4660}{40} = 116$$

The detector transformer has a step-up ratio of 1:3, therefore, the gain of the carrier amplifier must be:

$$A_c = \frac{116}{3} = 38.7$$

With the pneumograph gain scaled as shown above, a 15 ohm change in electrode impedance ($\Delta Z = 15$) will produce a 5 volt peak-to-peak output signal. If the total gain preceded the detector, the rectified carrier signal in the absence of respiration would be $E = 0.1 \times 4660 = 466$ volts which exceeds the dynamic range possible with a +28 volt supply and further this magnitude of voltage exceeds the capability of conventional transistors. For these reasons, the gain must be divided between a.c. and d.c. stages.

In order to d.c. couple the detector output signal to the d.c. amplifier, the average carrier signal level (without respiration) must be suppressed to zero volts. This can be accomplished using a summing network between the detector and a potentiometer which is energized from a stable d.c. source. By adjusting the potentiometer to a voltage level which is as much positive as the detector is negative, the output of the summing network is zero. This method is used in the design of the signal conditioners.

With the required carrier signal gain necessary to produce the desired output signal, any temperature induced circuit changes, hysteresis resulting from movement of vital organs, variations in electrode contact, and a variety of other artifacts causes large output level shifts to occur. This will necessitate rebalancing the potentiometer used to buck out the average detected carrier signal. As an example, assume that body movement caused by hysteresis resulting in a one ohm change in electrode impedance. The d.c. resulting signal would be:

$e_h = 1 \times 0.286 \times 10^{-3} \times 116 = 33.2 \times 10^{-3}$ volts at the input to the d.c. amplifiers. The d.c. amplifier has a gain of 40, therefore, the resulting change at the output of the d.c. amplifier would be:

$E_{dc} = 0.0332 \times 40 = 1.33$ volts and rebalancing of the bucking potentiometer would be required to reset the baseline.

The discussion outlined above illustrates the magnitude of the problem of designing a d.c. coupled pneumograph signal conditioner. However, if the unit is periodically rezeroed, baseline respiration data can be obtained which relates the output signal to the volume of air exchanged.

In the a.c. mode of operation, the coupling capacitors charge to levels determined by the magnitude of the detected carrier signal and block the changes discussed above provided the signal changes are slow compared to the system time constant.

The design, as shown on Schematic Diagram No. 102213, consists of an oscillator, electrode driver, carrier amplifier, detector, d.c. amplifier, negative 12 volt inverter, and a power line voltage regulator. Six terminals which are exterior to the case permit the operator to select either a.c. or a d.c. mode of operation. The desired mode of operation can be obtained by properly jumping the terminals in accordance with Table I, Drawing 102213. This signal conditioner was designed to operate from a supply voltage which can vary between +25.2 to +31 volts d.c.

Circuit Description

Each of the major parts of the pneumograph signal conditioner furnished under this program is described in the paragraphs that follow. A set of Operating Instructions, Spacelabs No. 102329, accompanied the two units delivered and should be used for proper operation of the unit.

Oscillator

A 50 + 5 kc oscillator consists of Q15 and its associated components. An LC type of oscillator was selected since it offered the best compromise with respect to simplicity, frequency stability, and minimum harmonic content in the output signal. This oscillator circuit is self-regulating. Tests have shown that the amplitude of the output signal varies approximately 0.1 volt per volt change in supply voltage. Positive feedback is injected at the emitter of Q15 and the large value of the emitter resistance, R65, maintains essentially unity gain over the entire range of the operating environment. This is evidenced by complete freedom from waveform clipping under all conditions of operation. The resistor capacitor network which is connected to the collector of Q15 establishes the d.c. bias, operating point, and the magnitude of the oscillator signal which is coupled to the electrode driver circuit.

Electrode Driver

The pneumograph electrodes are excited using a differential constant current source. The source consists of X_{C5}, X_{C6} and the secondary of transformer T1. It was found necessary to keep the load reflected from the primary of the electrode driver transformer T1 to R77 small enough so that changes in the electrode impedance are not reflected back as a variation in load to the oscillator. Transistors Q14 and Q25 are connected in a Darlington arrangement to reduce the effect of electrode load on the oscillators. Since the capacitive reactance of C5 and C6 at 50 kc is large, the electrode current is essentially independent of the electrode impedance. The voltage developed across the electrodes is differentially coupled to transistors Q12 and Q13.

Carrier Amplifier

A differential amplifier stage is used to reduce the effects of pickup (60 cycle) on the electrode leads and to maintain stray signal balance with respect to ground. The quiescent operating current of transistors Q12 and Q13 is designed to be approximately 50 microamperes. This value of quiescent current operating with 9 volts of base bias requires a large value of emitter resistance. Large values of emitter resistances provide adequate common-mode rejection without requiring transistor constant-current stages. The collector load impedance of Q12 consists of inductance L2 and capacitors C9 and C10 (anti-resonance at 50 kc). A tuned circuit is used as a collector load impedance to further reject common-mode signals from the output. This tuned circuit is shunted by R48 and the reflected load of transistor Q11. This value of shunt impedance reduces the operating circuit Q so that less than 1 db of amplitude change occurs over the operating frequency range of 50 + 5 kc. The single-ended output signal at the emitter of Q11 is coupled through an additional amplifier stage, Q10, and then to the detector transformer driver stage consisting of transistors Q6 and Q9. Another Darlington arrangement is used to reduce the reflected load of the detector transformer to the collector load impedance of amplifier Q10. This type of circuit configuration maintains adequate gain stability over the operating temperature range. The primary of the detector transformer, T2, is a.c. coupled to the emitter follower driver stage.

Detector

The secondary of transformer, T2, (1:3 ratio) is connected to a bridge rectifier circuit which detects the peak amplitude of the carrier signal. The modulated carrier is detected at the secondary of T2 by the use of a full wave bridge rectifier. Capacitor C15 at the output of the bridge rectifier is charged on each negative peak of the carrier signal. The time constant of the detector circuit is sufficiently short to follow the highest respiration rate. Field effect transistor Q18 is used in the a.c. mode of operation only as an impedance transfer stage. Q18 is connected in a source follower configuration and its output is capacitively coupled to the input to the d.c. amplifier. In the d.c. mode of operation, the output of the detector is summed with the voltage determined by the setting of potentiometer R78. R78 adjusted until the output of the summing network is zero (in the absence of a respiration signal). The output of the summing network is applied to the input of the d.c. amplifier.

D.C. Amplifier

The d.c. amplifier used in the design of this system has a gain of approximately 40. This amplifier has 0.5% gain stability, better than 1% linearity, and the output drift is less than + 50 mv over the operating temperature range. This amplifier is comprised of transistors Q1, Q2, Q3, Q4, and Q5.

-12 volt Supply

The d.c. amplifier requires -12 volts d.c. for its operation. System specifications require that the unit be capable of operating from a +28 volt supply. It was, therefore, necessary to provide a self-contained inverter power supply. The inverter is conventional in design and supplies approximately 34 volts peak-to-peak at 4 kc at the secondary of transformer T3. This signal is rectified using a full-wave-bridge rectifier. The output of the rectifier is filtered by capacitor C22. The filtered output is then zener-diode-regulated to -12 volts d.c. Since the d.c. amplifier is relatively insensitive to small changes in the negative supply voltage, a simple zener regulator can be used.

Power Regulator

It was necessary to provide a variety of supply voltages to obtain sufficient isolation between the various stages of the signal conditioner. The power regulator consists of zener diode Z5, transistor Q16, zener diode Z6, zener diode Z7, transistor Q17, zener diode Z8, and zener diode Z9.

Zener diode Z5 together with transistor Q16 is a roughing regulator which reduces the voltage change to the second stage regulator when the input voltage varies between +25 and +31 volts d.c. The output of the roughing regulator supplies voltage to zener diode Z6 (which supplies +20 volts to the -12 volt inverter) and also powers zener diode Z7 and transistor Q17. This zener diode-transistor combination provides a fairly well regulated source of + 15 volts for use in the carrier amplifier. In addition, the 15 volt supply powers the d.c. balance potentiometer from zener diode Z8 and is also reduced to +10 volts by Z9 for use in the d.c. amplifier. This series of regulators in conjunction with the various filter capacitors provides complete isolation between each section of the signal conditioner.

The pneumograph signal conditioner as shown on Schematic Diagram No. 102213, was designed to comply with the requirements of the performance specification. The feature of operation in either an a.c. or d.c. mode provides the capability for long term monitoring of respiration rate under the specified conditions of environmental temperature and in addition provides for short term experiments with an output signal which is relat... to the volume of air exchanged. This instrument provides the experimentor with a unit which is unique in the art of impedance pneumography.

4. SUMMARY

Under a contract with NASA, Ames Research Center, Spacelabs, Inc., carried out a research and development program directed toward the design and fabrication of an improved impedance pneumograph. The work grew out of some previous independent research, performed by Spacelabs, which examined the relationship

between the impedance measurement and volumetric changes during breathing. In the present program, a series of tests were conducted to provide information regarding the effects of several factors (including electrode placement, electrode design and body movement) on the various components of the impedance change. The information obtained during the study phase aided in the design of a new impedance pneumograph signal conditioner. Prototype units were fabricated and delivered to NASA, Ames Research Center, for further test and evaluation.

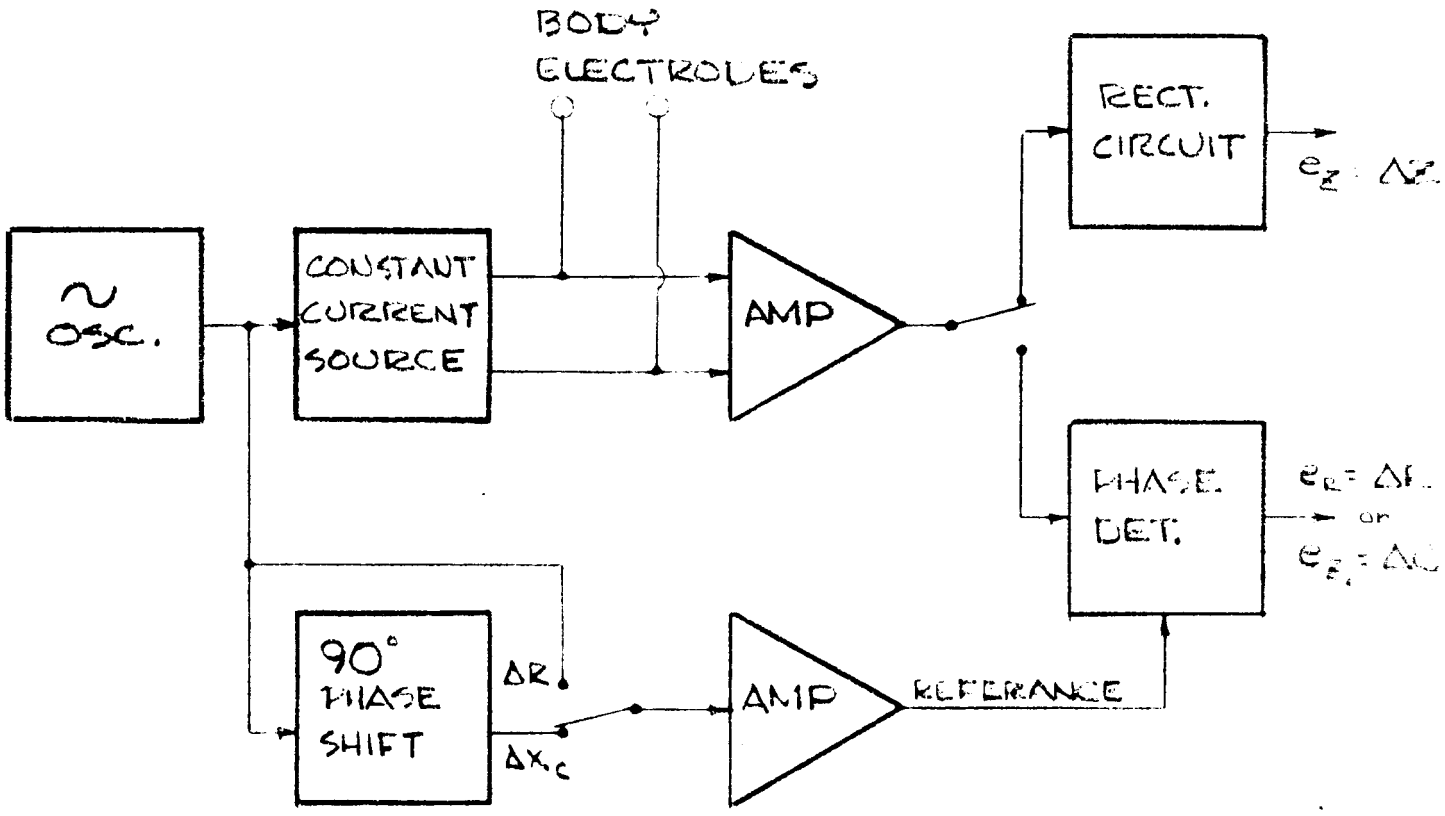

BLOCK DIAGRAM : CIRCUIT FOR SEPARATING COMPONENTS OF PNEUMOGRAPH IMPEDANCE CHANGE

FIG. 1

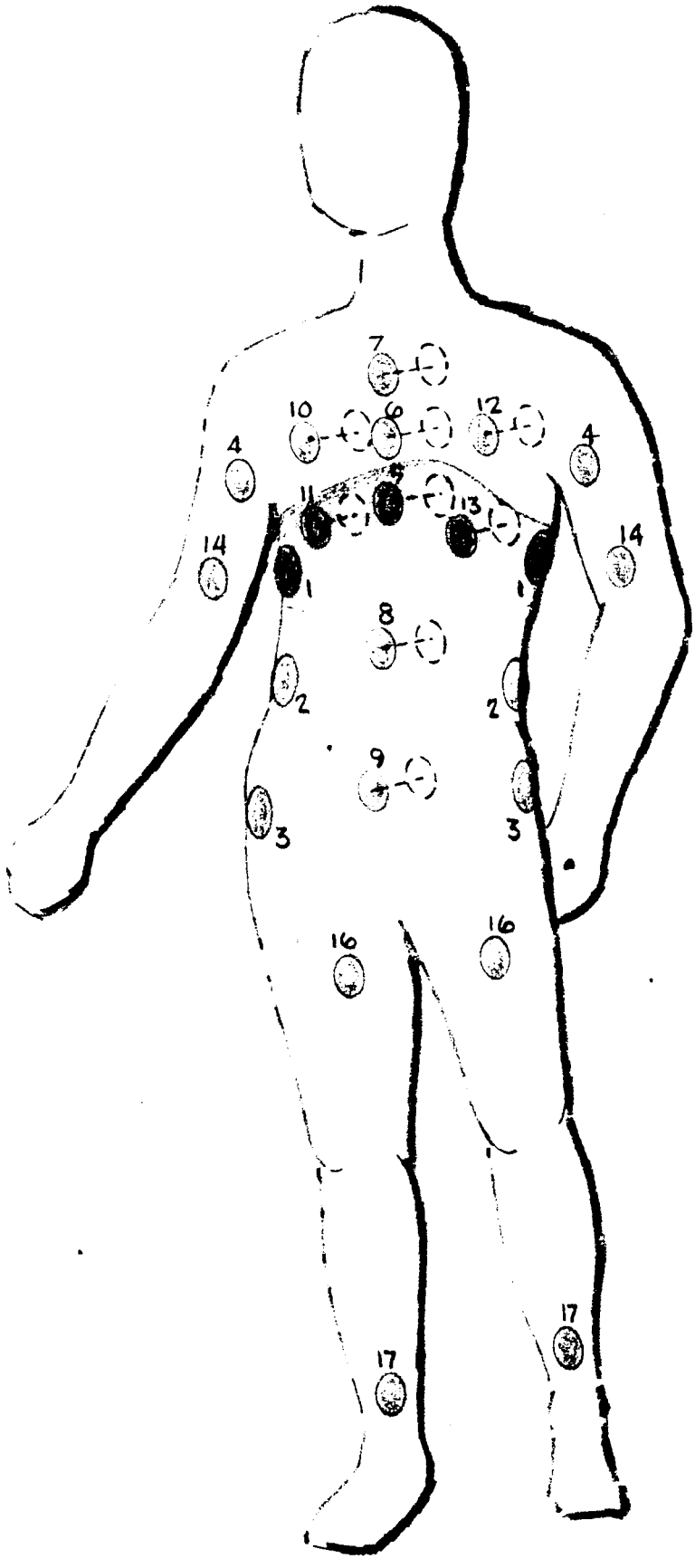

IMPEDANCE PNEUMOGRAPH ELECTRODE PLACEMENT

FIG. 2

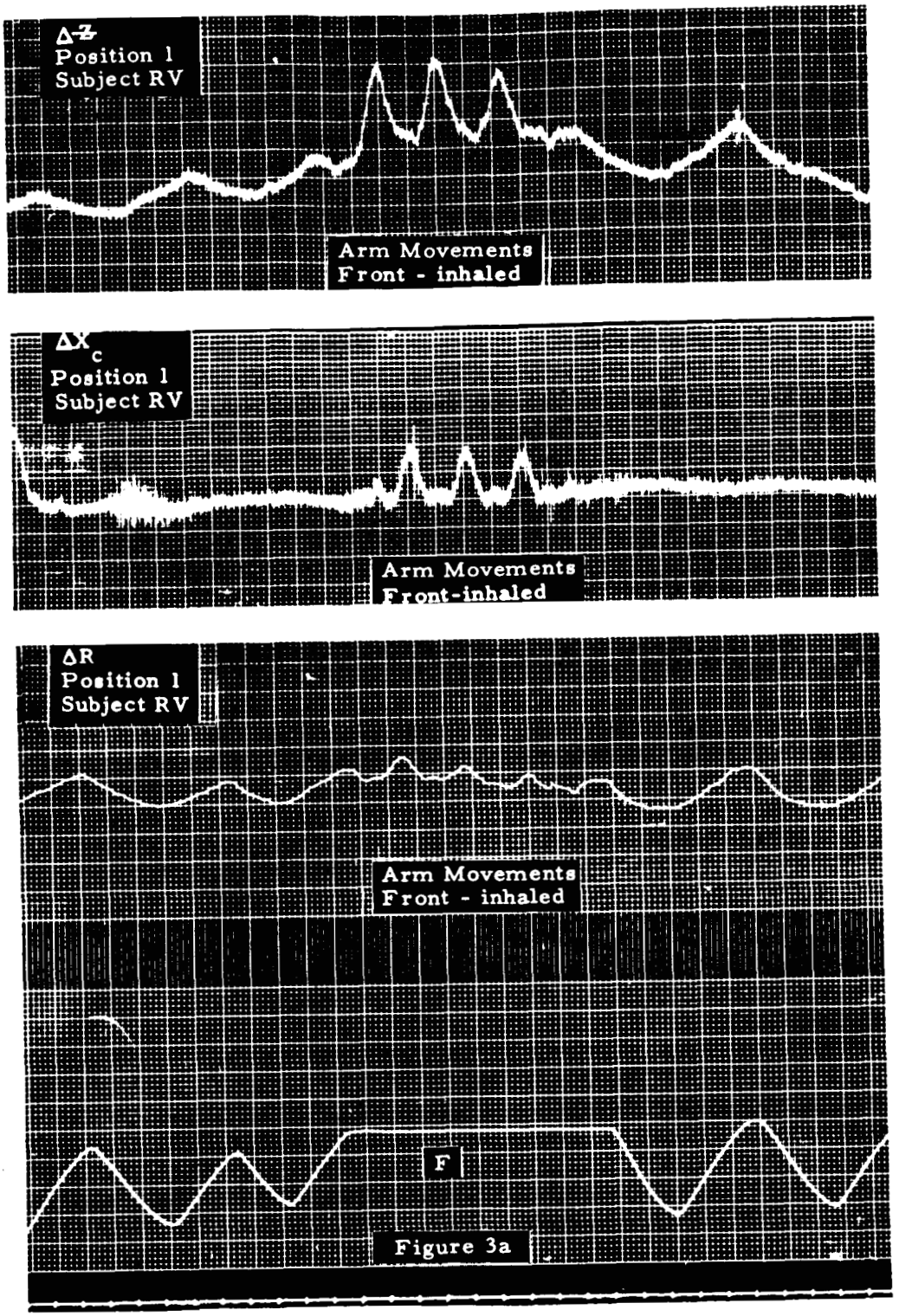

A COMPARISON OF IMPEDANCE COMPONENTS:
ARM MOVEMENTS IN FRONT OF THE BODY,
INHALATION SUSTAINED.

FIGURE 3

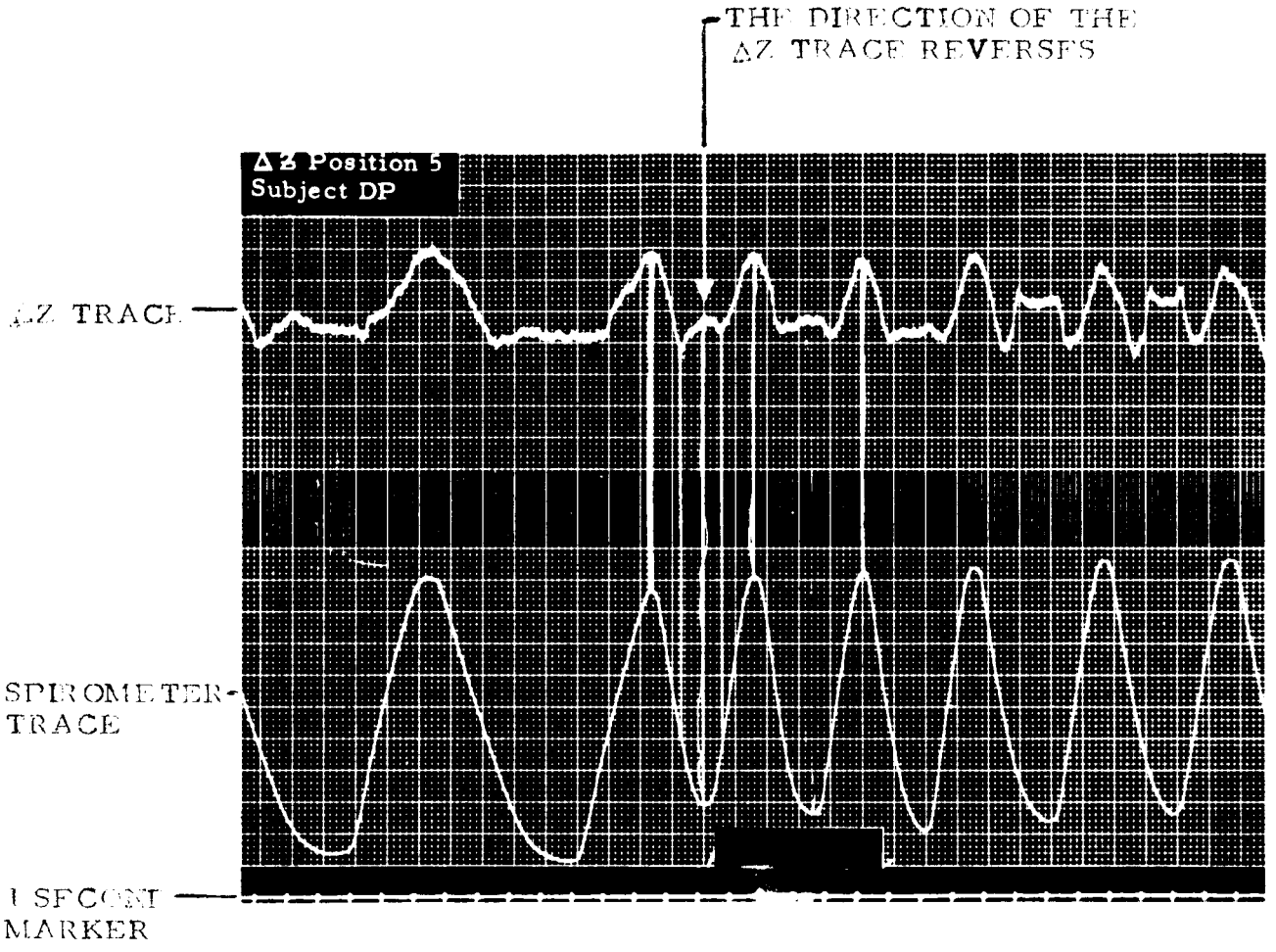

REVERSAL OF THE ΔZ TRACE DURING
BREATHING WITH THE IMPEDANCE ELECTRODES
PLACED ON THE CHEST AND BACK

FIGURE

Spacelabs, Inc.
15521 LANARK ST.
VAN NUYS, CALIFORNIA
DWG NO
10279

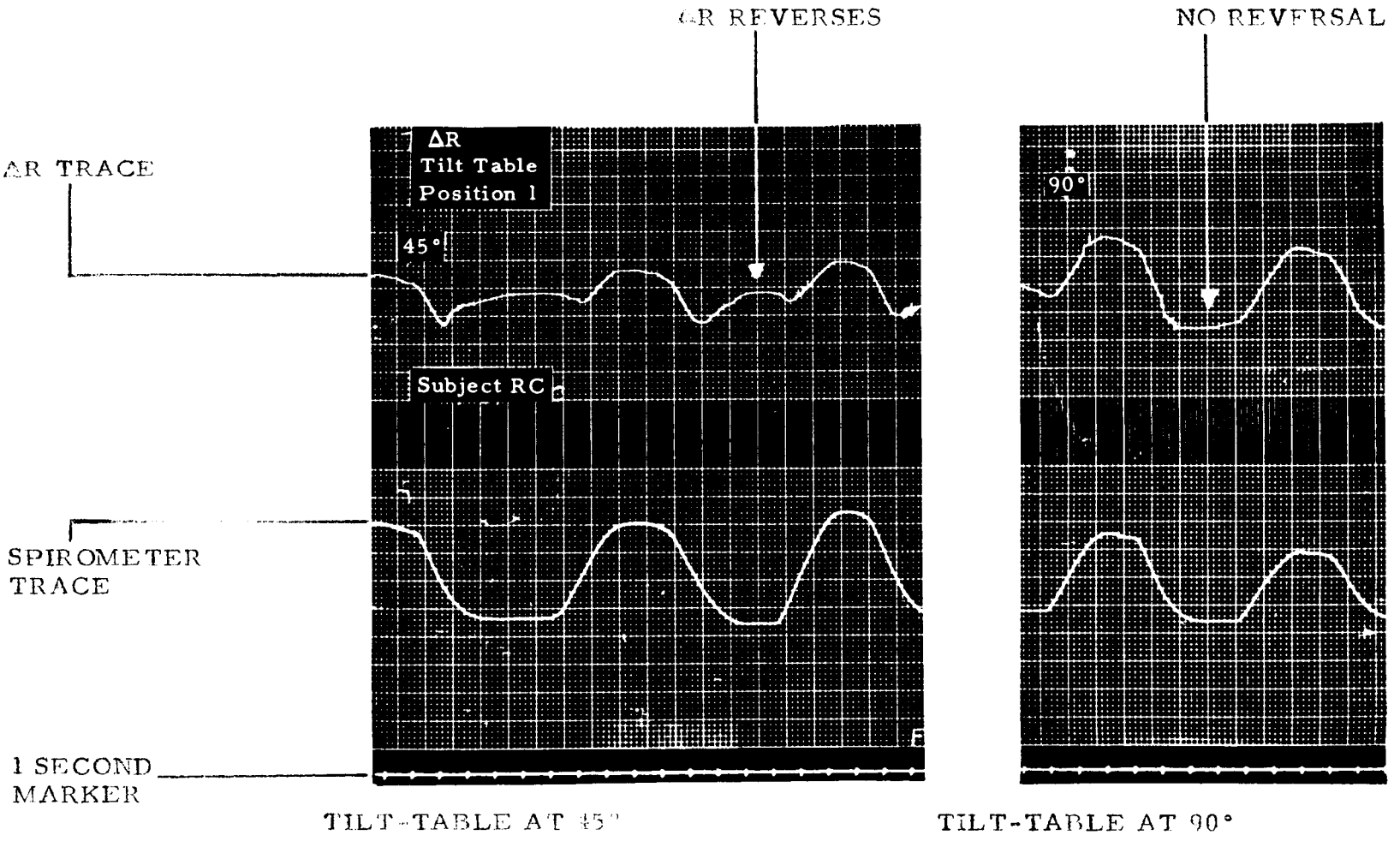

DISAPPEARANCE OF THE REVERSAL PHENOMENON
AS THE SUBJECT IS ROTATED TO THE HORIZONTAL

FIGURE 5

Spacelabs, Inc.
15521 LANARK ST.
VAN NUYS, CALIFORNIA
DWG NO

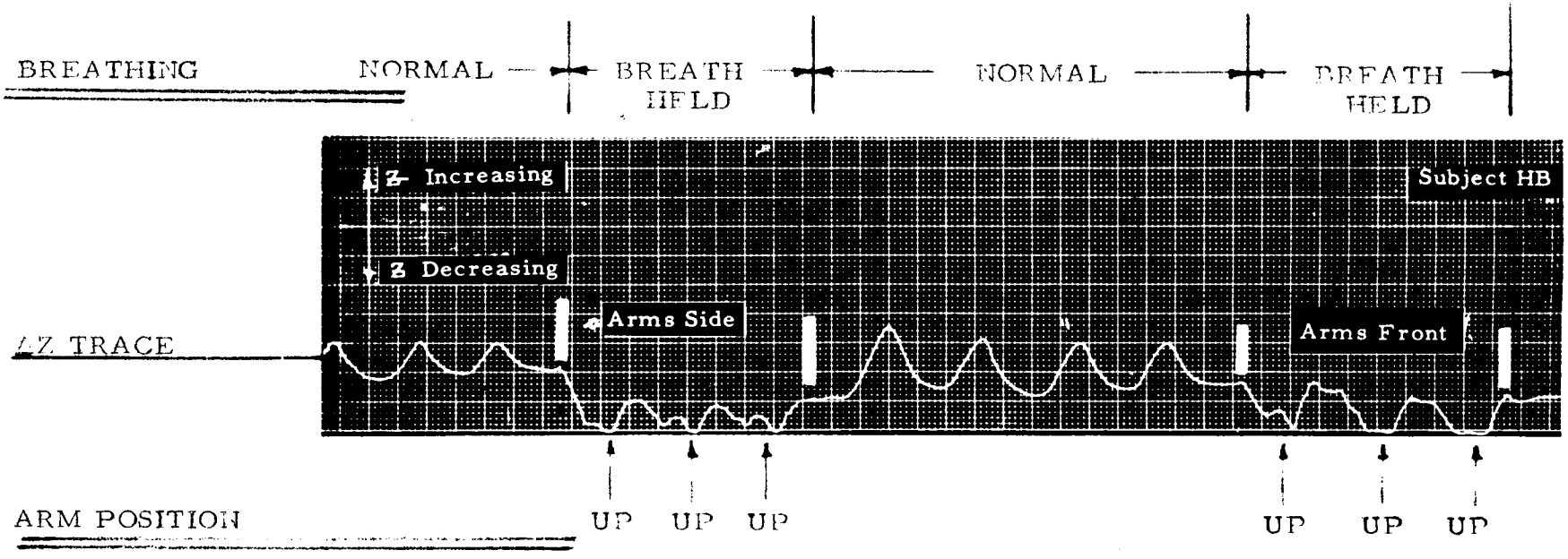

A DEMONSTRATION THAT ΔZ DECREASES AS THE ARMS ARE RAISED WHEN THE IMPEDANCE ELECTRODES ARE LOCATED ACROSS THE LIVER

FIGURE 6

APPROXIMATE
ELECTRODE
POSITION

BACK: 2nd LUMBAR
VERTEBRAE

FRONT: MID-AXILLARY,
BETWEEN 7th
AND 8th RIBS

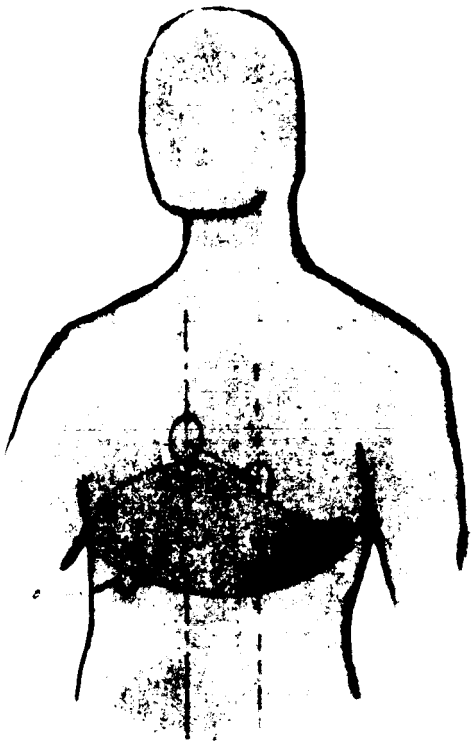

LIVER

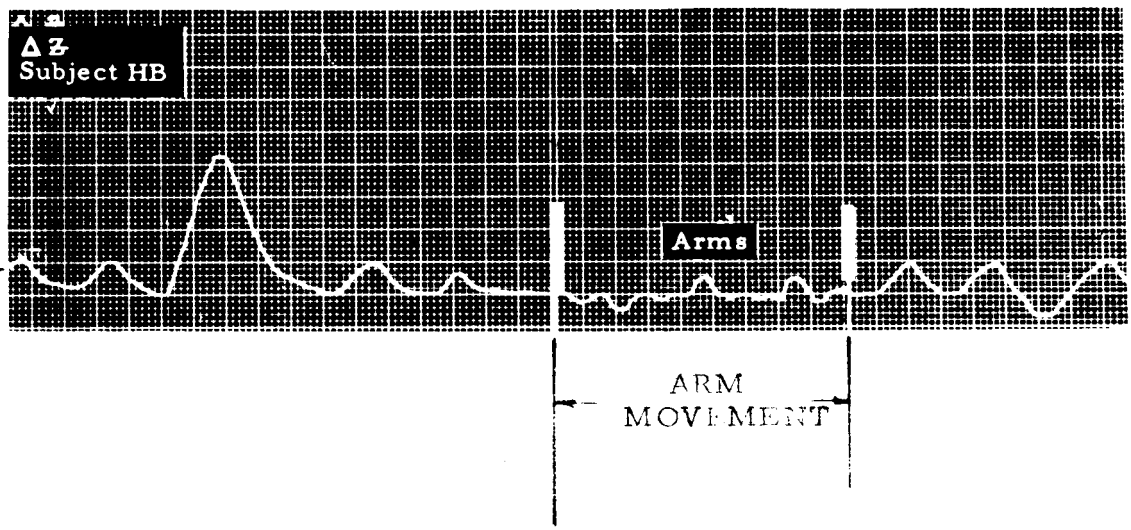

ΔZ TRACE

A DEMONSTRATION THAT ARTIFACT DURING ARM MOVEMENT IS REDUCED IF THE ELECTRODES ARE PROPERLY PLACED WITH RESPECT TO THE LIVER

FIGURE 7

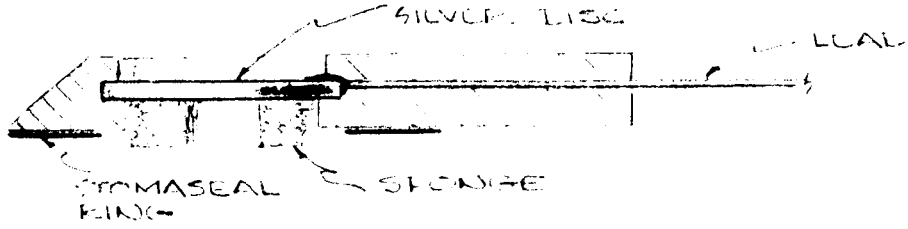

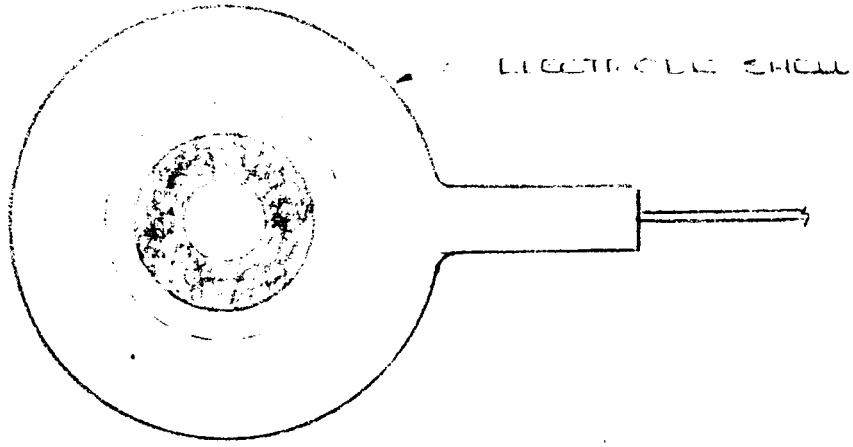

IMPEDANCE PNEUMOGRAPH ELECTRODE

FIG. 8

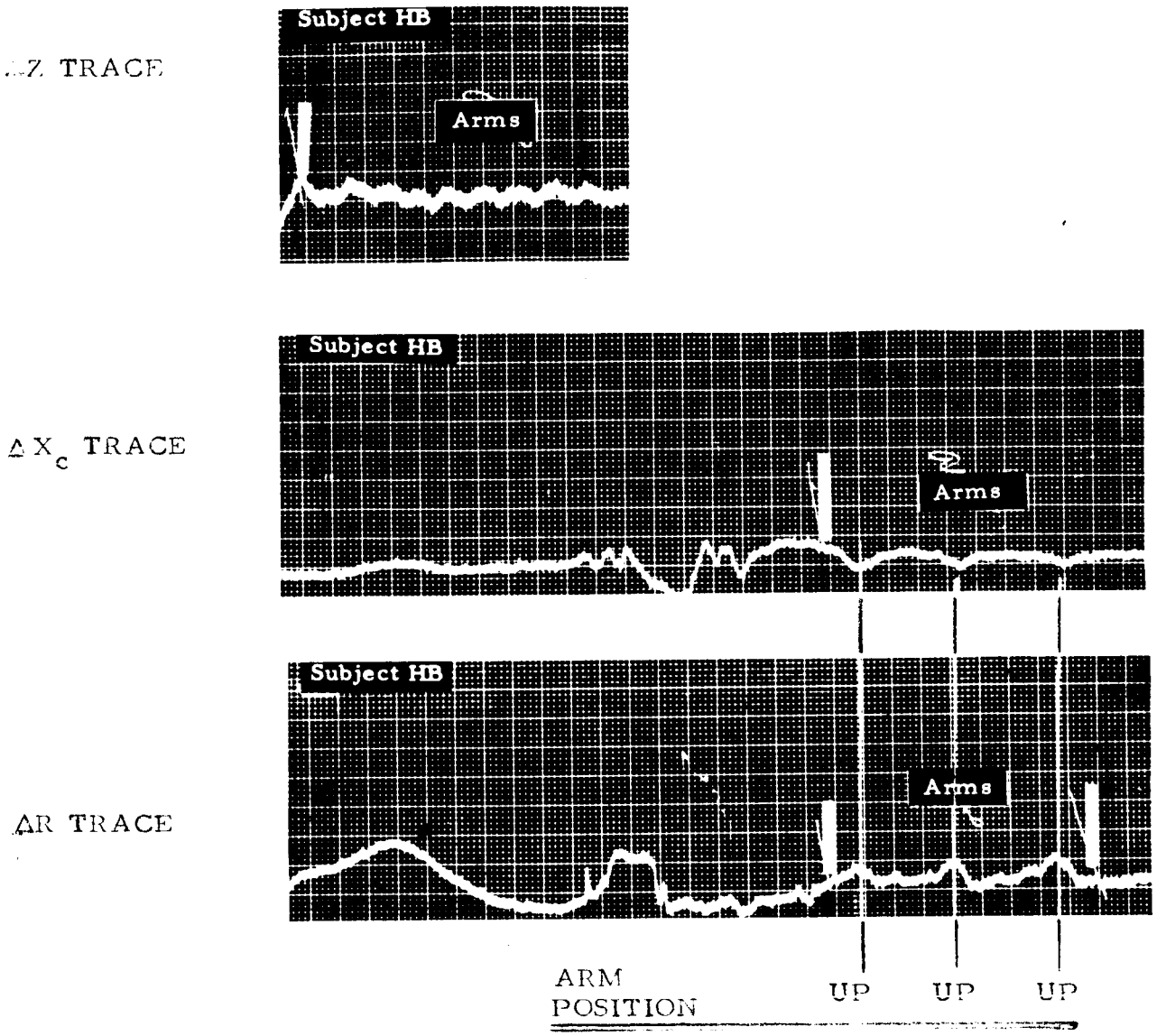

THE EFFECT OF ARM MOVEMENT
ON THE COMPONENTS OF IMPEDANCE

FIGURE 9

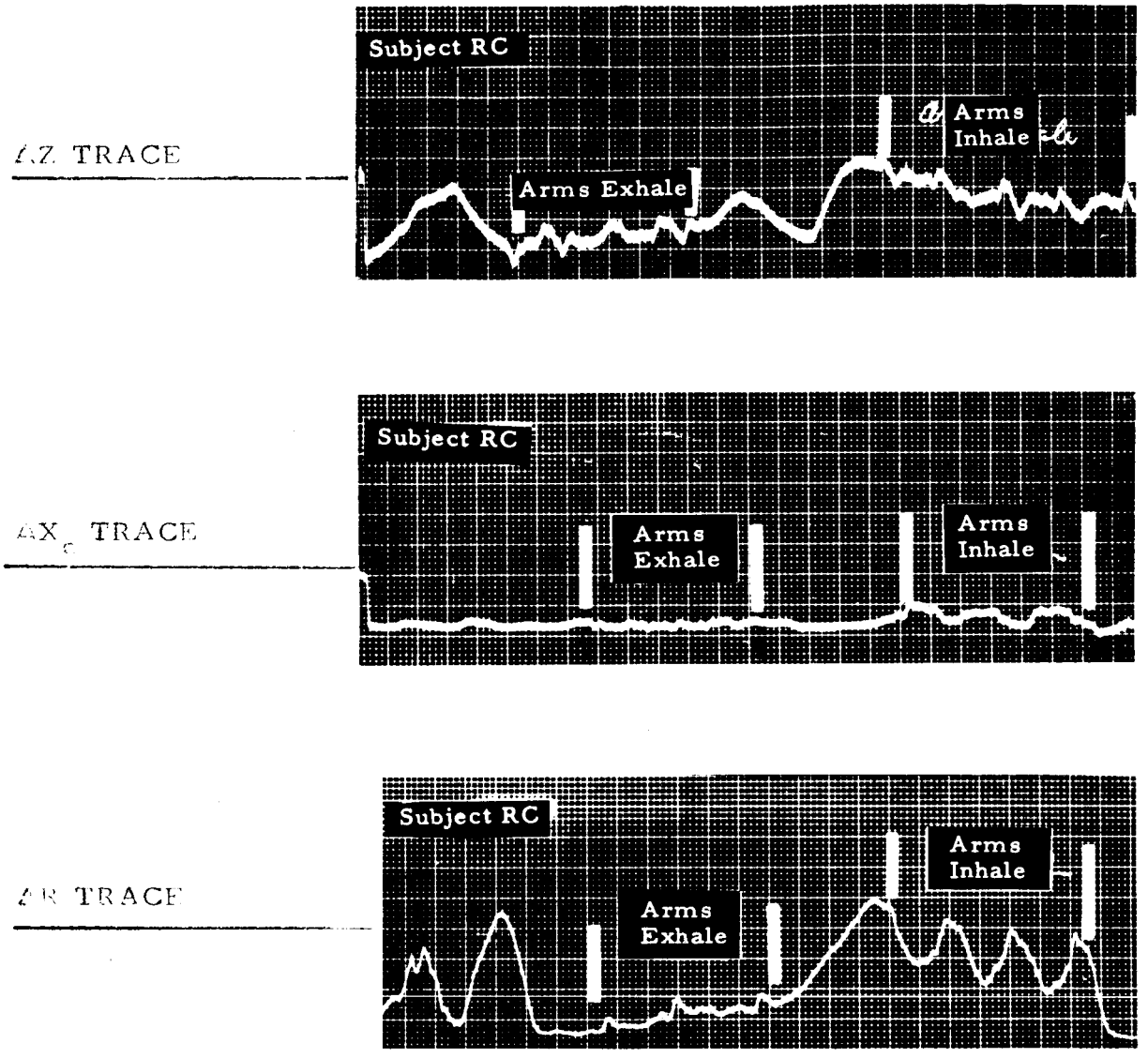

THE EFFECT OF ARM MOVEMENT DURING SUSTAINED EXHALATION AND INHALATION ON THE COMPONENTS OF IMPEDANCE

FIGURE 10

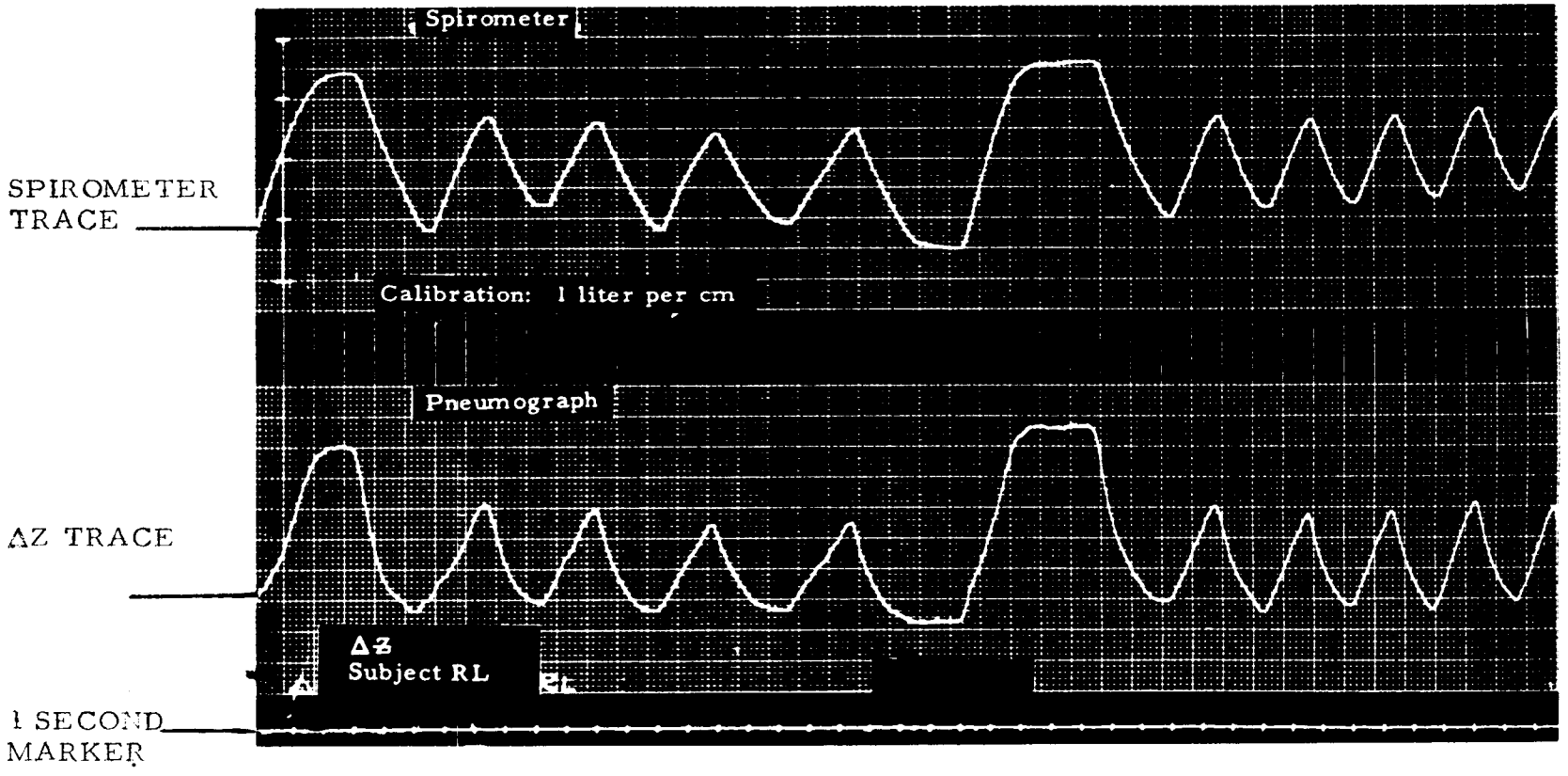

SIMULTANEOUS RECORDING OF SPIROMETER AND IMPEDANCE PNEUMOGRAPH OUTPUTS WITH IMPEDANCE ELECTRODES IN RECOMMENDED POSITION

FIGURE 11

APPENDIX A

(DWG. NO. 101056)

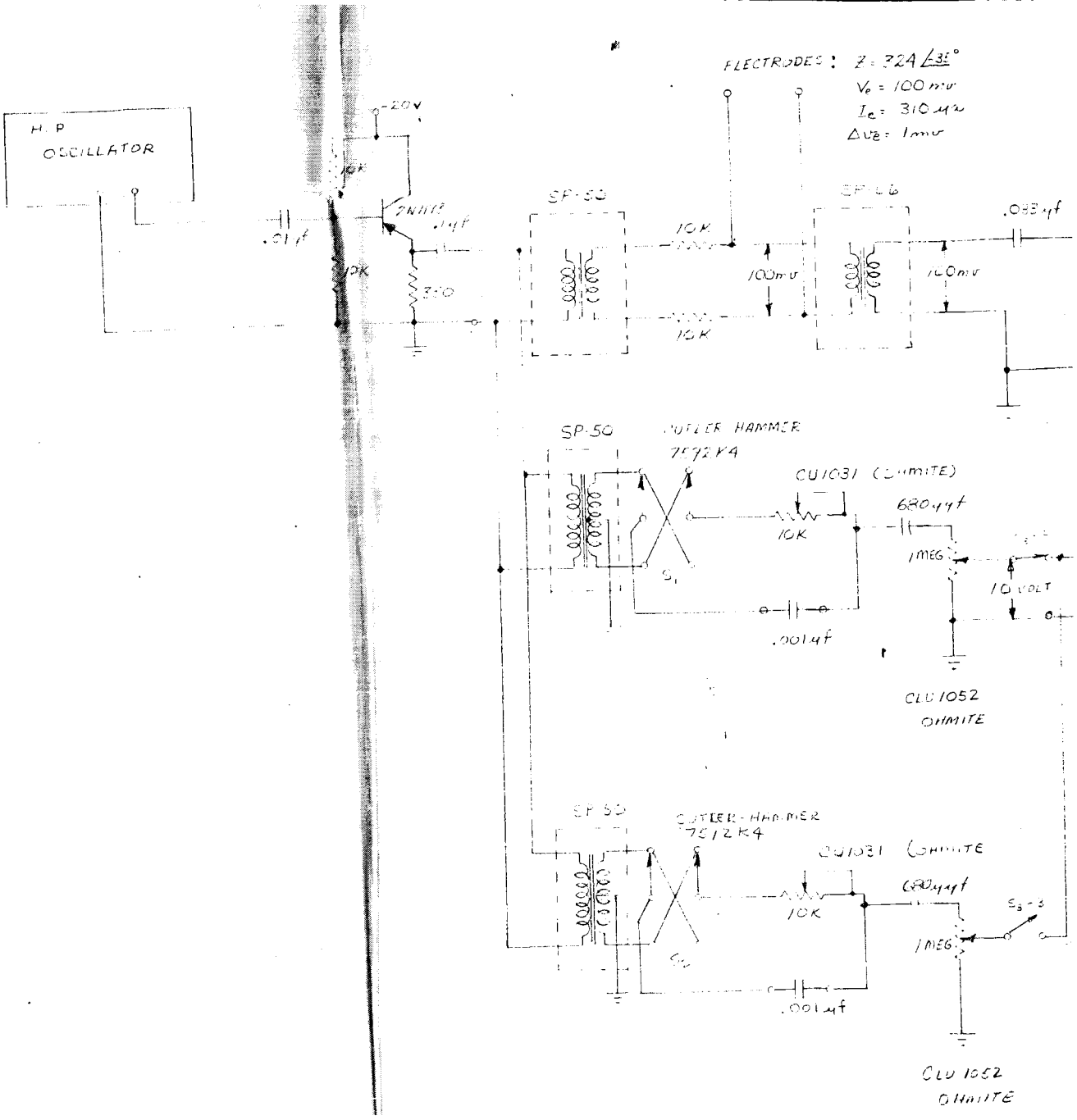
ELECTRODES : Z = 324 ∠35°
Ve = 100 mv
Ie = 310 μa
Δve = 1mv
H. P
OSCILLATOR
-20V
10K
2N1132
.1μf
.01μf
10K
330
SP-50
10K
100mv
10K
SP-50
.083μf
100mv
SP-50
OUTLER HAMMER
7512K4
CU1031 (OHMITE)
680μμf
10K
1MEG
10 VOLT
.001μf
CLU 1052
OHMITE
SP-50
OUTLER-HAMMER
7512K4
CU1031 OHMITE
680μμf
10K
1MEG
.001μf
CLU 1052
OHMITE

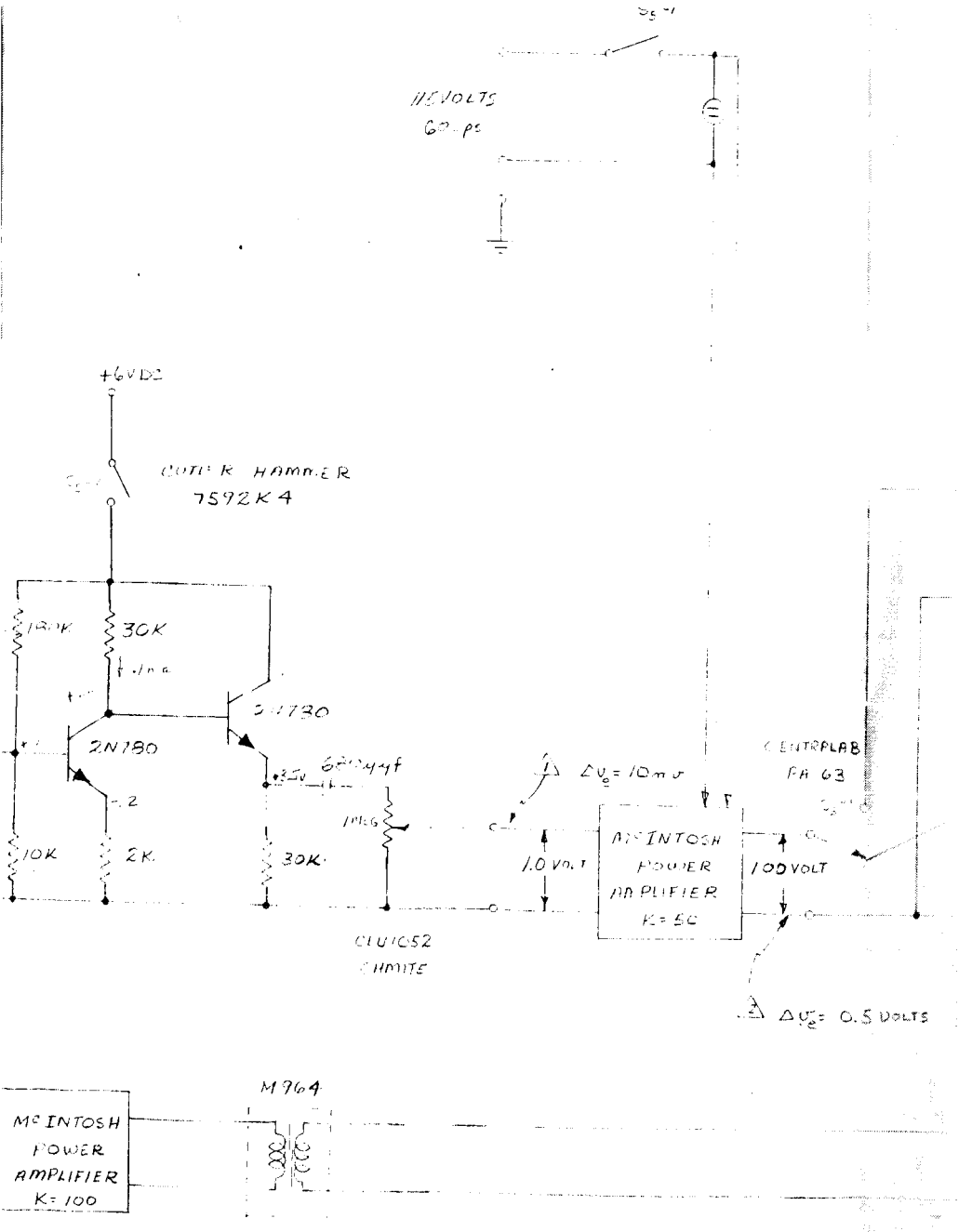
115 VOLTS
60 ~ ps
+6 VDC
CUTLER HAMMER
7592K4
30K
1 m a
2N1730
2N180
.2
10K
2K
30K
1 MEG
CLU1052
SMITE
ΔEe = 10 m v
1.0 VOLT
McINTOSH
POWER
AMPLIFIER
K = 50
100 VOLT
CENTRALAB
PA 63
ΔEe = 0.5 VOLTS
M964
McINTOSH
POWER
AMPLIFIER
K = 100

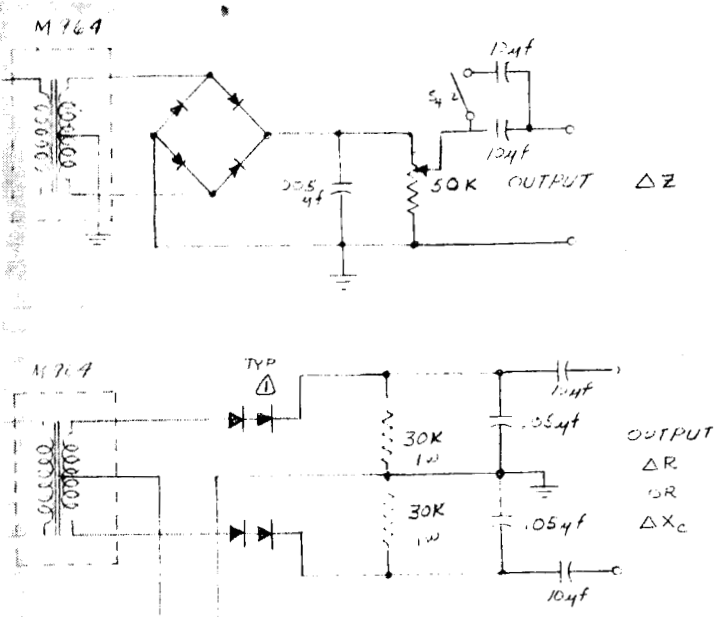

NOTE:

1. ALL DIODES ARE IN345
2. ALL RESISTORS ARE 1/2 WATT, 10%

DRAFT	[illegible]	12/4/70
DESIGNER		
STRESS & WEIGHT		
CHECKER		
DESIGN ENG	[illegible]	12/4/70
MFG ENG		
STDS ENG		
PROJ ENG		

TITLE: SCHEMATIC
PNEUMOGRAPH
PHASE DETECTOR
7170

LAYOUT | RELEASE DATE
SCALE | WT ACT LB | WT CALC LB

Spacelabs, Inc.
15521 LANARK ST.,
VAN NUYS, CALIFORNIA

DWG NO 101056
REV A
SHEET 1 OF 1

APPENDIX B

(DWG. NO. 102213)

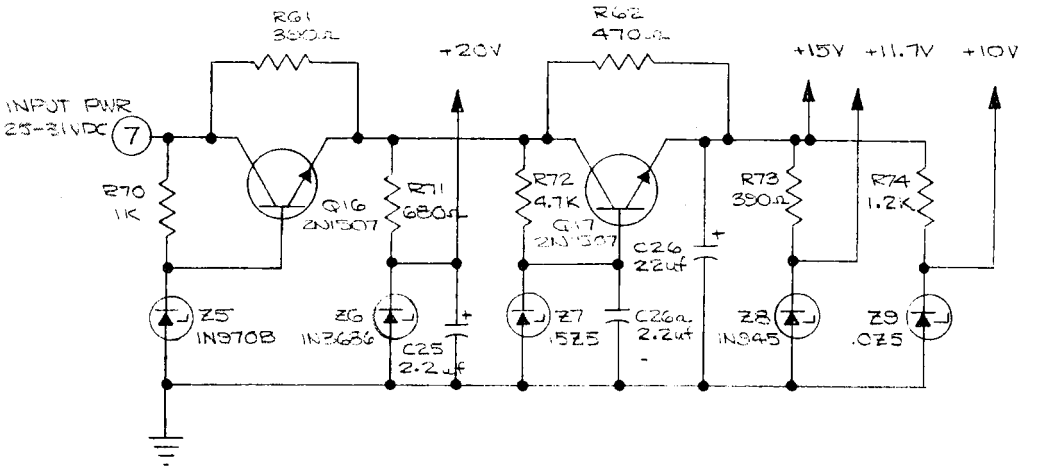
RG1
39Ω 2L
R62
470Ω 2L
+20V
+15V
+11.7V
+10V
INPUT PWR
+25-31VDC
7
R70
1K
Q16
2N1507
R71
680Ω
R72
4.7K
Q17
2N1307
C26
22uf
R73
390Ω
R74
1.2K
Z5
IN970B
Z6
IN2686
C25
2.2uf
Z7
.525
C26a
2.2uf
Z8
IN945
Z9
.035

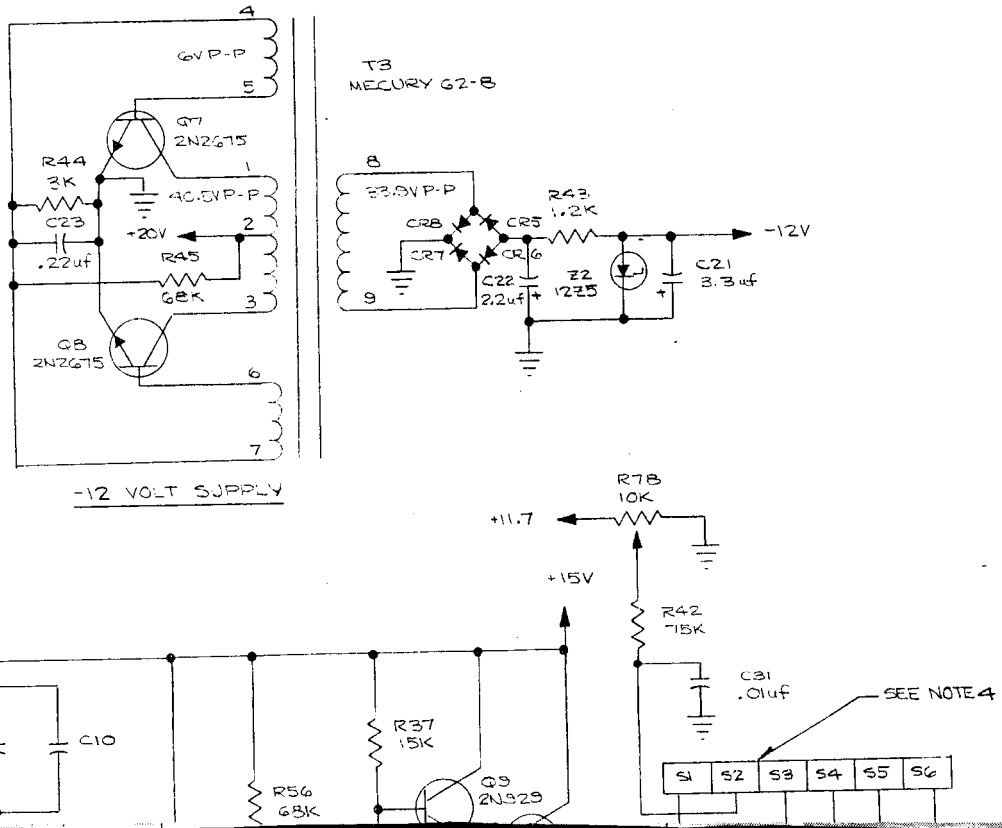
4
6V P-P
5
Q7
2N2675
R44
3K
1
40.5V P-P
C23
.22uf
+20V
2
R45
68K
3
Q8
2N2675
6
7
-12 VOLT SUPPLY
T3
MECURY 62-8
8
33.9V P-P
R43
1.2K
CR8
CR5
-12V
CR7
CR6
C22
2.2uf
Z2
12Z5
C21
3.3 uf
9
R78
10K
+11.7
+15V
R42
75K
C31
.01uf
SEE NOTE 4
L2
C9
C10
R56
68K
R37
15K
Q9
2N929
S1
S2
S3
S4
S5
S6
C30
.22uf

REVISIONS						
DISPOSITION CODE:		1 MAY BE REWORKED 4 NOW SHOP PRACTICE	2 CANNOT BE REWKD. 5 PARTS MADE OK	3 RECORD CHANGE		
REV SYM	WORD CODE	DESCRIPTION	MFG EFF	SHIP CODE PART	SHIP CODE ASSY	APPROVAL & DATE
—		PRODUCTION RELEASE	5-8-64			

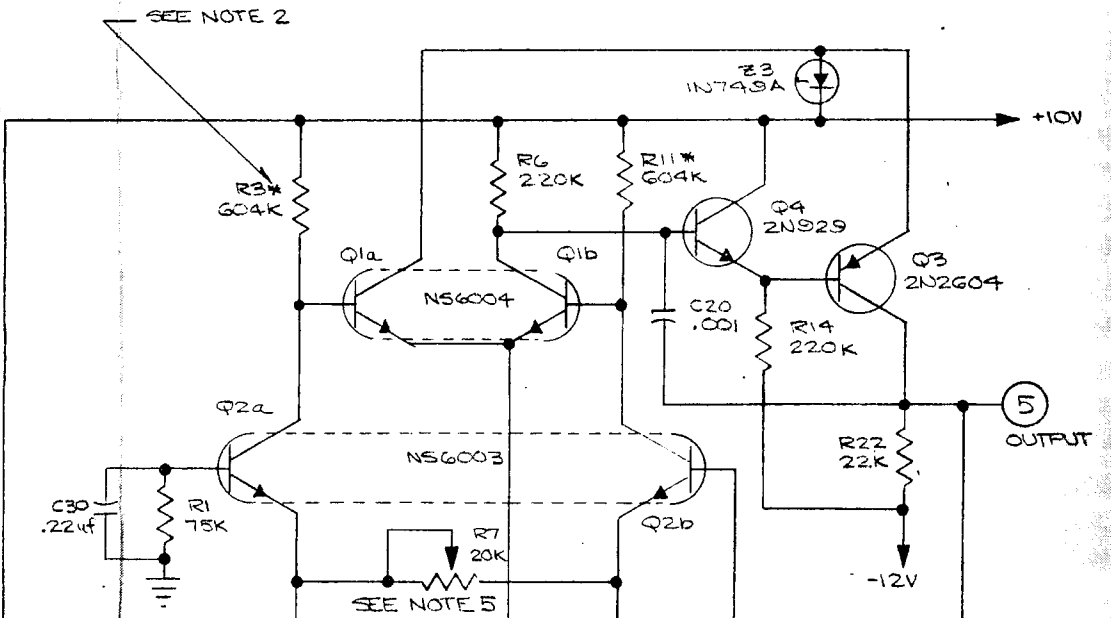

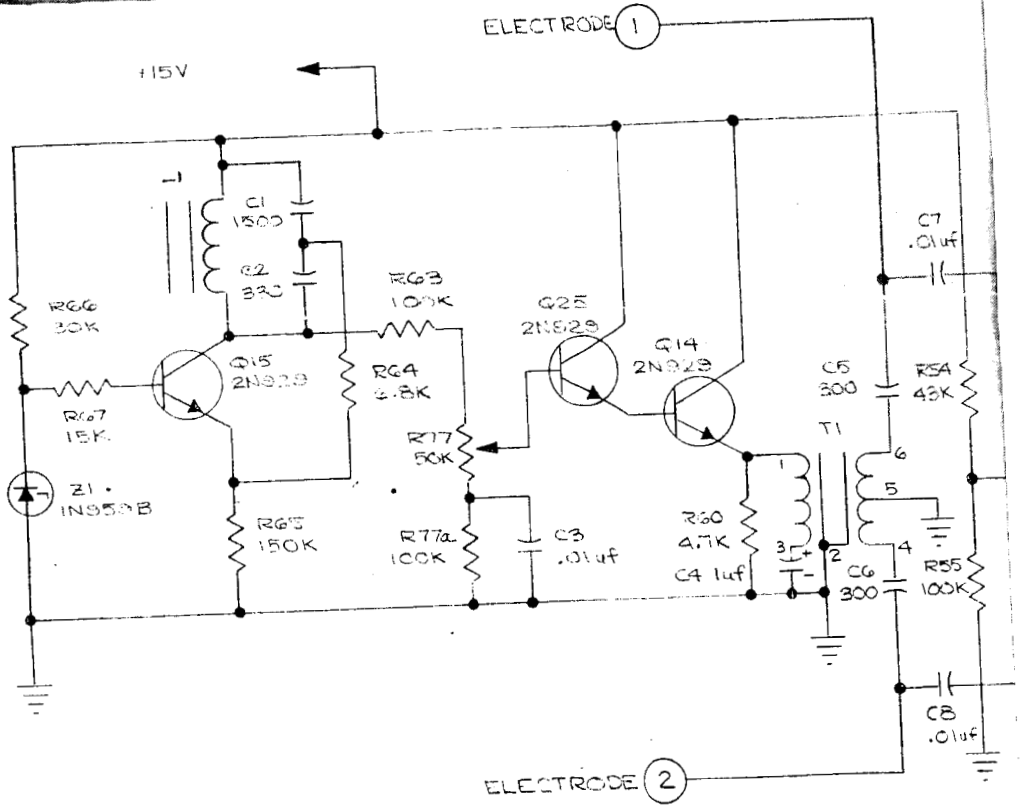

NOTES: (UNLESS OTHERWISE SPECIFIED)

1. COMPONENTS WITH VALUES NOT SHOWN WILL BE SELECTED DURING ELEC. TEST.
2. * ASTERISK INDICATES METAL FILM RESISTOR
3. RESISTORS ARE 1/4W ± 5% CARBON
4. OUTPUT CAN BE AC OR DC, FOR SWITCHING SEE TABLE I
5. SELECT FOR 2.5 VDC AT 10 MA OUTPUT IN AC MODE OF OPERATION

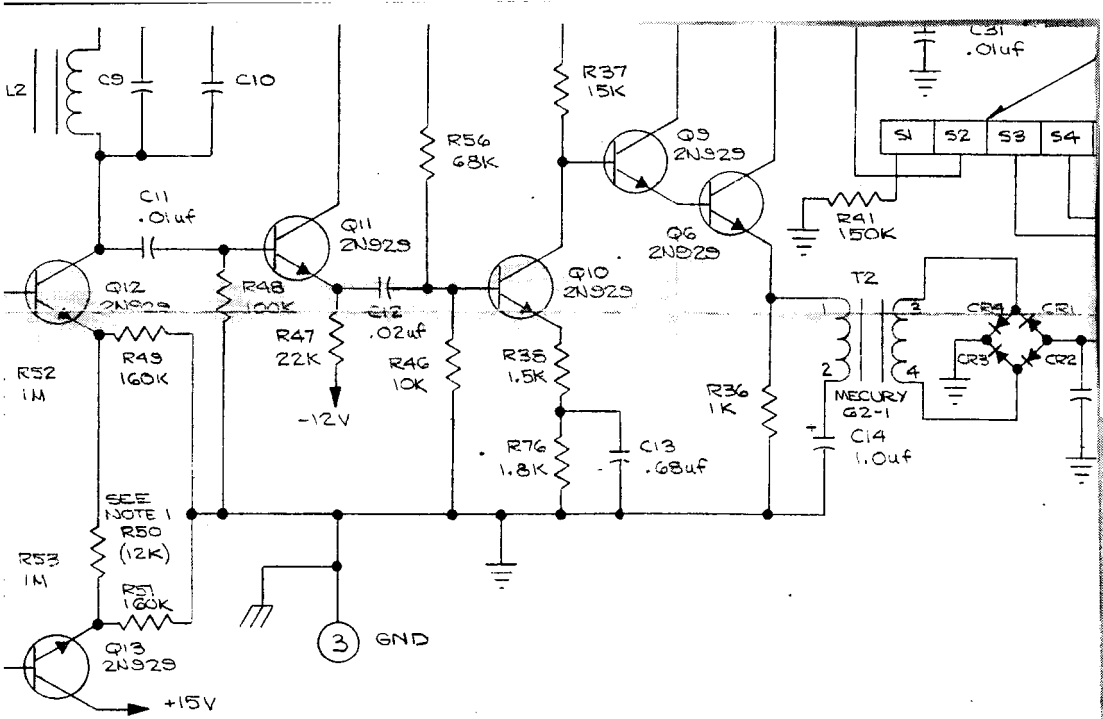

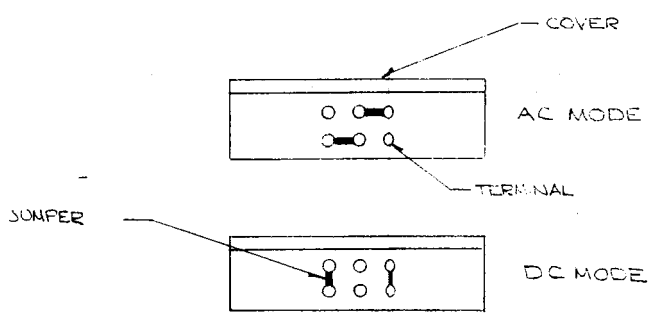

TABLE I
(TERMINALS EXT. TO CASE)

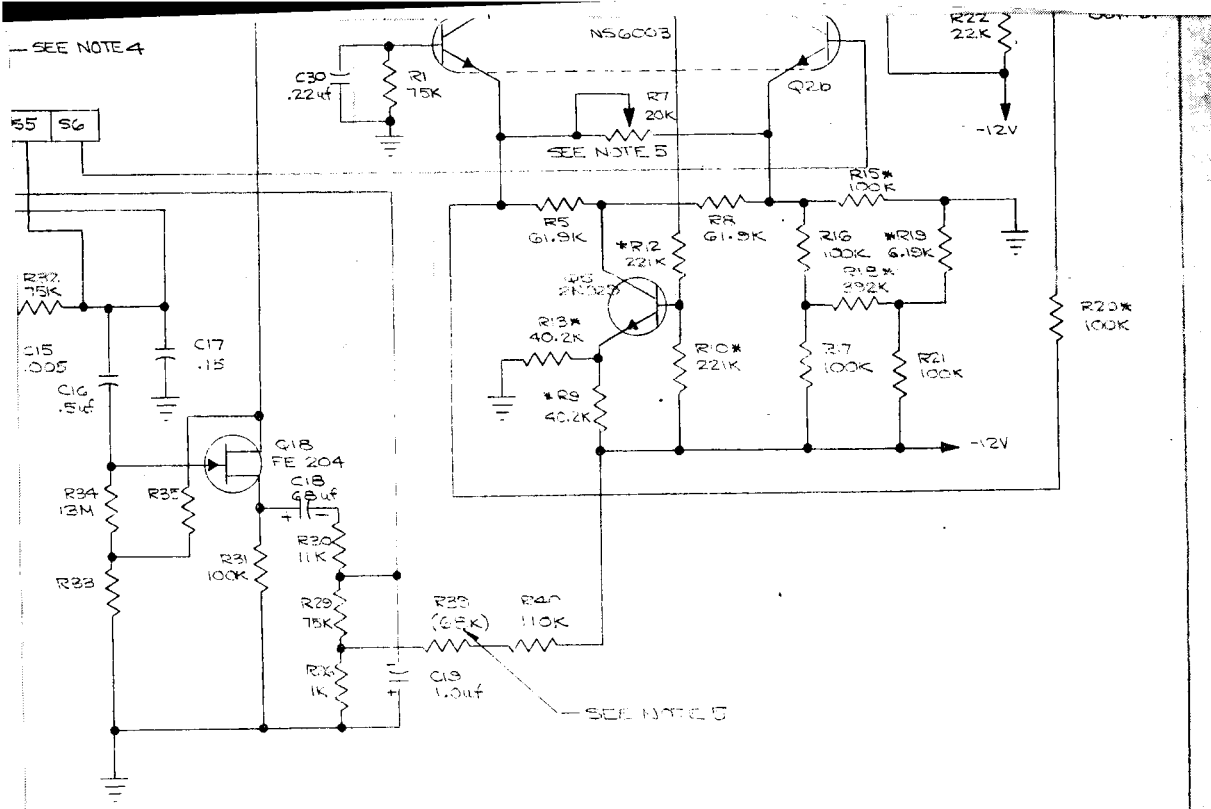

LIST OF MATERIAL

QTY PER ASSY	ITEM	PART NO	DESCRIPTION	MATL	MATL SPEC	ZONE

PART NO	EFF	MOD NO	NEXT ASSY	NEXT ASSY	FINAL ASSY	APPLICATION	QTY REQ

CALCULATED WT LB

PART NO

REFERENCE TO SIMILAR DWG

DWG SIZE D

UNLESS OTHERWISE SPECIFIED
DIMENSIONS ARE IN INCHES
TOLERANCES ARE:
.XX — ± .03 | .XXX — ± .010 | X° — ± 0° | ± 30'
WEIGHT IS IN LBS & TENTHS
ALL FINISHED SURFACES 125 PER MIL-STD-10
MFR PER SPEC
TOLERANCE SYMBOLS PER MIL-STD-8
ELECTRICAL SYMBOLS PER MIL-STD-15
MECHANICAL SYMBOLS PER MIL-STD-17
WELDING SYMBOLS PER MIL-STD-19

DRAFT	Thase	3/6/69
DESIGNER	VAA	4-1-69
STRESS & WEIGHT		
CHECKER		
DESIGN ENG		
MFG ENG		
STDS ENG		
PROJ ENG	Hebert	4-1-69

TITLE
SCHEMATIC DIA
PNEUMOGRAPH,
NASA, AMES

LAYOUT
RELEASE DATE 4-18-69
SCALE
WT ACT LB
WT CALC LB
SHEET 1 OF 1

Spacelabs, Inc.
15521 LANARK ST.
VAN NUYS, CALIFORNIA

DWG NO 102213
REV

APPENDIX C

BIBLIOGRAPHY

1. Altman, Philip L., Gibson, John F. Jr. M.D., Wang, Charles C., "Handbook of Respiration," WADC-TR-58-352, ASTIA AD 155 823, August 1958.

2. Baker, L. E., "Impedance Spirometry," 14th Southwestern IRE Conference, April 1962.

3. Bartlett, R. G. Jr., Brubach, H. F., Trimble, R. C., Specht, H., "Airway Resistance Measurement During Any Breathing Pattern in Man," Journal of Applied Physiology, 14(1):89-96, January 1959.

4. Bartlett, R. G. Jr., Bruach, H. F., Specht, H., "Demonstration of Aventilatory Mass Flow During Ventilation and Apnea in Man," Journal of Applied Physiology, 14(1):97-101, January 1959.

5. Bartlett, R. G. Jr., Moss, Arthur J., "Observation on the Pneumotachocardiogram," U.S. Naval School of Aviation Medicine, Project MR 005.13-7004 Sub-Task 7, Report No. 1.

6. Dantzig, George B., DeHaven, James C., Cooper, Irwin, Johnson, Selmer M., DeLand, C. Edward, Kanter, Herschel E., Sams, Crawford, M.D. "A Mathematical Model of the Human External Respiratory System," ASTIA AD 246 199, September 28, 1959.

7. Feder, Walter, "Silver-Silver Chloride Electrode as a Nonpolarizable Bioelectrode," Journal of Applied Physiology, 18(2):397-401, March 1963.

8. Fenn, W. O., Otis, A. B., Rahn, H., "Studies in Respiratory Physiology," WADC TR 6528, August 1951.

9. Geddes, L. A., Hoff, H. E., "The Measurement of Physiological Events by Impedance."

10. Goldensohn, E. S., Zablow, L., "An Electrical Impedance Spirometer," Journal of Applied Physiology, 14(3):463-464, May 1959.

11. Hall, F. G., Salzano, John, "Effect of Body Posture on Maximal Inspiratory and Expiratory Stroke Volume," ASTIA AD 212 319, March 1959.

12. Long, Ernest Croft, Hull, Wayland E., Gebel, Emile L., "Respiratory Dynamic Resistance," Journal of Applied Physiology, 17(4):609-612, July 1962.

13. Lucchina, G. G., Phipps, C. G., "An Improved Physiologic Electrode," ASTIA AD 281 262, June 1962.

14. Marko, Adolf, "Monitoring Unit for Heart and Respiration Rate," ASTIA AD 246 141, August 1960.

15. McCal, Charles B., Hyatt, Robert E., Nobel, Frank W., Fry, Donald L., "Harmonic Content of Certain Respiratory Flow Phenomena of Normal Individuals," Journal of Applied Physiology, 10(2):215-218, March 1957.

16. McCally, M., Barnard, G. W., Robins, K. E., Marko, A. R., "An Impedance Respirometer," AMRL TDR-63-45, June 1963.

17. Schaeffer, J. P., Morris" Human Anatomy, The Blakiston Company, 1953 Eleventh Edition.

18. Sosnow, M., Ross, E., "Electrodes for Recording Primary Bioelectric Signals," ASD TR 61-437, September 1961.

19. Watson, John F. Capt. USAF, MC, Cherniack, Neil S. Capt. USAF, MC, Zechman, Fred W., Jr. PhD., "Respiratory Mechanics During Forward Acceleration," WADD TR 60-594, September 1960.